Acta Geodyn. Geomater., Vol. 6, No. 2 (154), 135–142, 2009

EFFICIENCY OF INDIVIDUAL CRL STATIONS IN SEISMIC MONITORING OF THE WESTERN GULF OF CORINTH

Jaromír JANSKÝ *, Jiří ZAHRADNÍK and Vladimír PLICKA

Department of Geophysics, Faculty of Mathematics & Physics, Charles University, V Holešovičkách 2, 180 00 Praha, Czech Republic, +420 221 911 444, fax +420 221 911 214
**Corresponding author's e-mail:* jansky@seis.karlov.mff.cuni.cz

(*Received* February 2009*, accepted* April 2009)

ABSTRACT
We study the efficiency of individual stations of the CRL seismic network in recording the seismic activity in the western Gulf of Corinth, Greece. The stations are located on both the northern and southern coast of the Gulf. The study is based on 5027 earthquakes recorded in 2001, separated into three groups, the southern, central and the northern one. The events were located using the HYPO71PC algorithm. It is shown that the stations significantly differ in their monitoring ability.

KEYWORDS: Gulf of Corinth, Corinth Rift Laboratory seismic network

INTRODUCTION

The western part of the Gulf of Corinth is seismically very active (e.g. Bernard et al., 2006). Interesting geodynamic processes and the related earthquake, tsunami and landslide hazards call for detailed studies of this area. Therefore, in addition to standard monitoring of this area by the regional Greece seismic network of the National Observatory of Athens, NOA, and the recently established Hellenic Unified Seismic Network, HUSN, accurate locations, and especially locations of weak events, need additional, specifically targeted local networks. The western Greece has been monitored by the University of Patras (the PATNET and PSLNET networks). In the Corinth Gulf, several networks have been also operated by the University of Athens (e.g. RASMON, CORSA). Detailed investigations in the western Corinth Gulf have been accomplished within the Corinth Rift Laboratory (CRL) Project. For this purpose, the CRL seismic network (CRLNET) was deployed on the northern and southern coasts of the Gulf of Corinth (Lyon-Caen et al., 2004). The distribution of individual CRL stations is shown in Figure 1.

A further development of any observing systems is impossible without thein efficiency analysis. As a rule, even in a relatively small region, individual seismic stations might significantly differ as regards the number of events to which the stations contributed in the location process. The reasons are numerous, including local geology, instrument installations, digitizer performance, etc. Although each of the effects can be investigated separately, the most practical approach is to estimate their overall significance through statistical evaluation of a representative data set. Therefore, the objective of this paper is to evaluate efficiency of the CRL stations through the analysis of abundant data recorded in 2001. The results might facilitate important decisions such as which stations need to be kept, upgraded (e.g. real-time transmitted), improved (e.g. put in a vault), or closed.

DATA AND METHOD

In the year 2001 a total of 7932 events were detected by the CRL in the western part of Corinth Gulf. From these events 6253 were recorded at least at three stations. For routine event locations, the CRL uses a layered structural model, hereinafter referred to as CRLM. This model resulted from a seismological experiment carried out in 1991 (Rigo et al., 1996). The CRLM is an average 1-D model composed of 6 homogeneous layers over a homogeneous halfspace with the MOHO at a depth of 30 km. The v_P/v_S velocity ratio is 1.80. We used the same model and located (for purposes of this paper) 6149 events using the HYPO71PC (Lee and Valdés, 1989) algorithm.

To analyze the station efficiency, we need a set of well recorded events. We select the events meeting the following criteria: epicentral distance of the nearest recording station must be less than 15 km; both standard error of the epicenter (ERH) and focal depth (ERZ) must be less than 5 km; the root mean square error of time residual (RMS) must be less than 1 sec. (For definition of ERH, ERZ and RMS, see HYPO71PC manual.) These criteria have been satisfied by 5027 events.

The events have an irregular spatial distribution (Fig. 1); most of them have been connected with the seismic activity in the vicinity of Aegion town (Fig. 1). We therefore divide the epicenters into three parts, namely the southern, central and northern one,

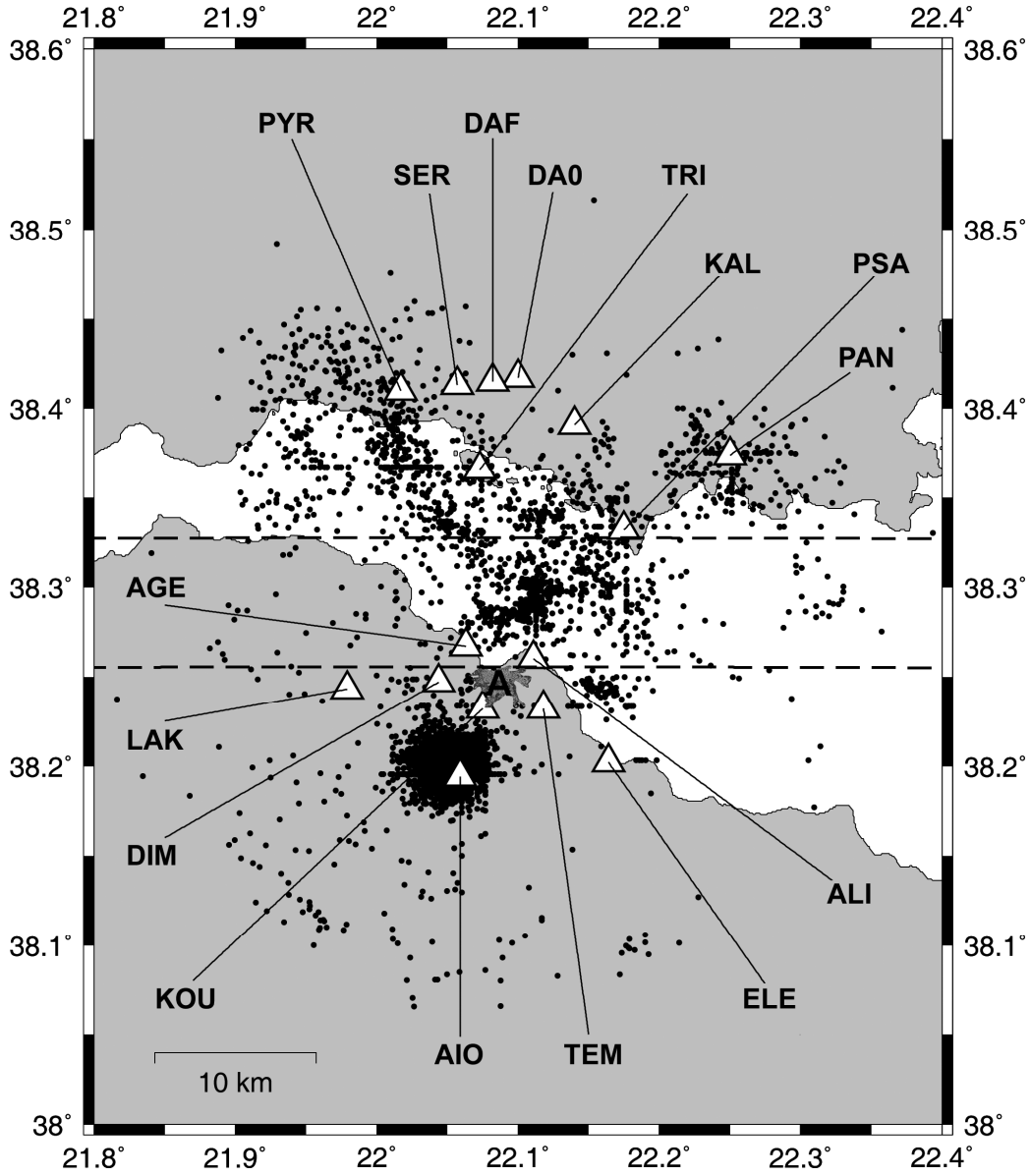

Fig. 1 The western part of the Gulf of Corinth with CRL stations and epicenters of 5027 events. The southern, central and northern parts are delineated by dashed lines. The position of the town of Aegion is also shown by a letter A.

with 3132, 787 and 1108 events, respectively. Later, for better comparison, the results will be normalized to compensate for unequal number of events in the three regions.

The following analysis is made for each of the three groups separately: We multiply each onset by its quality factor, associated to each phase by the interpreter, mainly according to the phase reading accuracy (1, 0.75, 0.50, 0.25 and 0, see the HYPO71 manual), and sum these numbers over all phases recorded by a given station. Thus we obtain the weighted sum of onsets. Further, we divide this weighted sum by the total number of located events, thus getting the so-called weighted recording percentage. This weighted recording percentage shows the monitoring efficiency of a given station.

RESULTS - SOUTHERN PART

For the southern part of dataset we have 20776 *P*-wave onsets (from them 16507 at the southern stations) and 17036 *S*-wave onsets (from them 13246 at the southern stations). This represents on average 6.63 *P*-wave and 5.44 *S*-wave onsets per event. The weighted recording percentage of the whole set of southern events, recorded on individual CRL stations for the *P*- and *S*-waves, is given in Figure 2. A quite

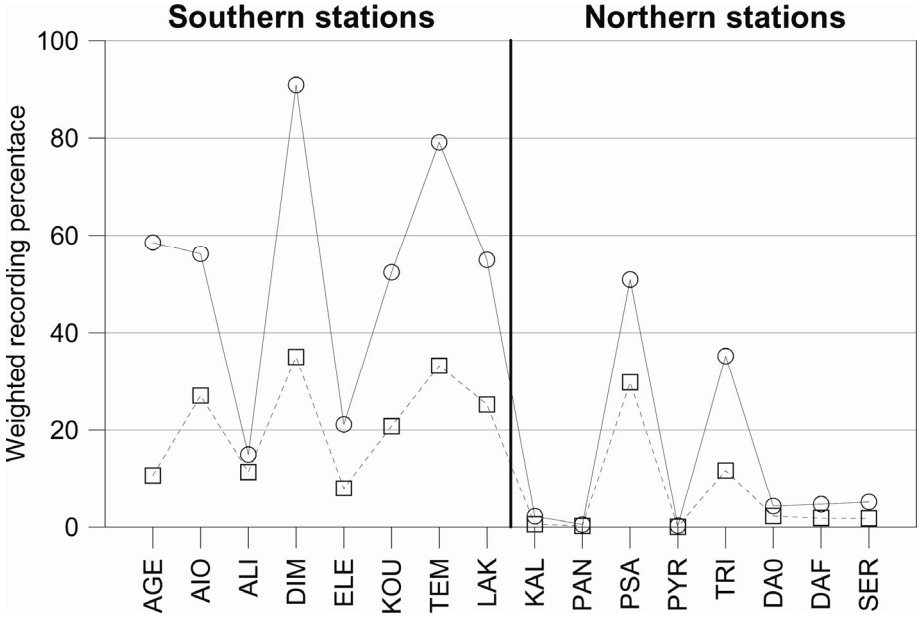

Fig. 2 Weighted recording percentage of all located events in the **southern part** of dataset, shown for individual CRL stations separately for the *P*-wave (circles and solid line) and *S*-wave (squares and dashed line) onsets. The most efficient stations are DIM and TEM.

large difference in the efficiency of individual stations from the point of view of *P*-waves onsets is seen from this figure. On average, we observe a dominant efficiency of southern stations, as expected. But even within the group of the southern stations there are significant differences. Stations DIM and TEM have the best performance, followed by stations AGE, AIO, KOU and LAK with a medium efficiency. Stations ALI and ELE recorded only small portion of the events. Two of the northern station (PSA, TRI) manifest the medium efficiency as well. All other northern stations have only negligible efficiency. The behavior of individual stations from the point of view of *S*-wave onsets follows the *P*-wave results with just a few differences (the relative level is, of course, lower than for the *P*-waves, due to the lower number of S-wave readings and often lower quality factor association). All together, for the southern set of events, we get the following average parameters with their mean deviation: distance of the nearest station 2.92±1.55 km, RMS=0.11±0.04 s, ERH=0.91±0.36 km, ERZ=0.72±0.31 km, azimuthal gap=227±35^{o} and average depth 7.57±1.14 km.

RESULTS - CENTRAL PART

For the central part of dataset we have 5026 *P*-wave onsets (from them 3339 at the southern stations) and 4026 *S*-wave onsets (from them 2501 at the southern stations). This represents in average 6.38 *P*-wave and 5.12 *S*-wave onsets per event. The weighted recording percentage from the whole set of central events, recorded on individual CRL stations for the *P*- and *S*-waves, is given in Figure 3. Due to the position of events between the northern and southern stations, both groups of stations have basically the same ability to record the events. But a quite large difference in the efficiency of individual stations is observed, see Figure 3. The northern stations PSA and TRI are the best for both the *P*-wave and *S*-wave onsets from group of stations. All other northern stations have only negligible efficiency. Practically all the southern stations, including ELE and ALI manifest medium efficiency for both the *P*- and *S*-wave onsets that is approximately on the same level as for the southern events. For the central set of events we get the following average parameters with their mean deviations: distance of nearest station 4.65±1.75 km, RMS=0.10±0.05 s, ERH=0.68±0.46 km, ERZ=0.80±0.48 km, azimuthal gap=162±43^{o}. and average depth 7.34±1.15 km.

RESULTS - NORTHERN PART

For the northern part of dataset we have 7987 *P*-wave onsets (from them 5022 at the southern stations) and 6182 *S*-wave onsets (from them 3403 at the southern stations). This represents in average 7.21 *P*-wave and 5.58 *S*-wave onsets per event. The weighted recording percentage from the whole set of northern events, recorded on individual CRL stations for the *P*- and *S*-waves, is given in Figure 4. The general behavior is the same as that of the central part, with just a few exceptions only. In other words, to a certain surprise, the contribution of southern station is not suppressed for the northern part of epicenters,

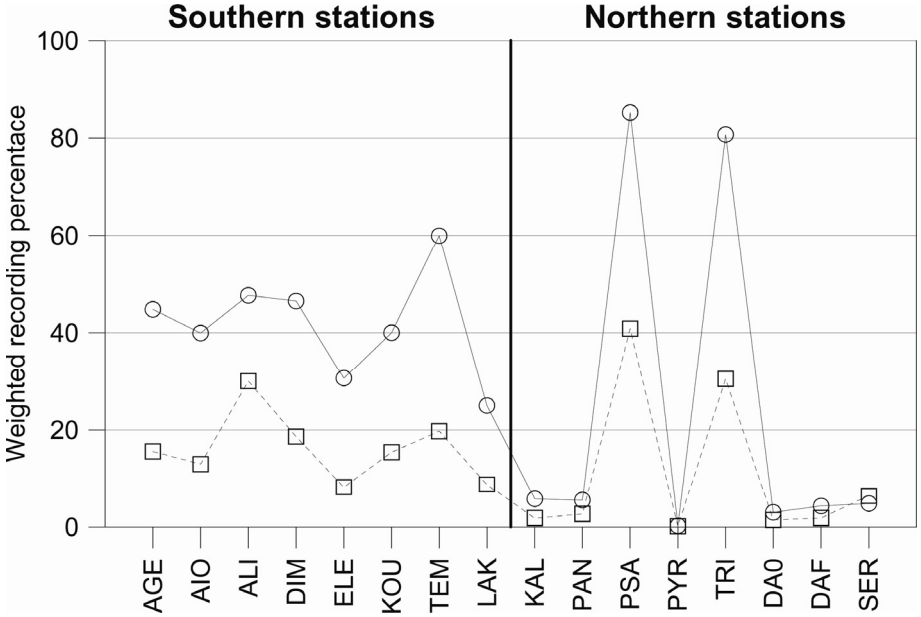

Fig. 3 As in Figure 2, but for the **central part** of dataset. The most efficient are the stations PSA and TRI.

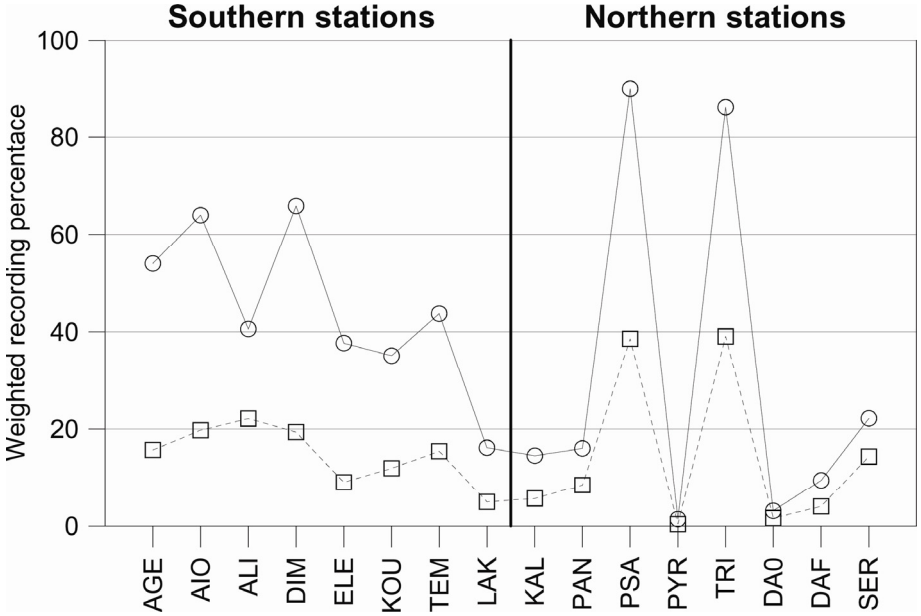

Fig. 4 As in Figure 2, but for the **northern part** of dataset. The most efficient stations are again the stations PSA and TRI.

while the importance of northern stations is just slightly larger compared to the central part. For the northern set of events we get the following average parameters with their mean deviations: distance of nearest station 5.87±3.01 km, RMS=0.14±0.06 s, ERH=1.21±0.59 km, ERZ=1.16±0.58 km, azimuthal gap=241±54^{o} and average depth 9.10±1.55 km.

RESULTS - EFFICIENT COMBINATIONS OF THE SOUTHERN AND NORTHERN STATIONS

It is also of interest to analyze how the successful locations were distributed between the southern and northern stations (as a whole), without addressing the individual stations (just considering if it belongs to the southern or northern coast). Therefore, we calculate the frequency of successful locations at a number of the station combinations: e.g.

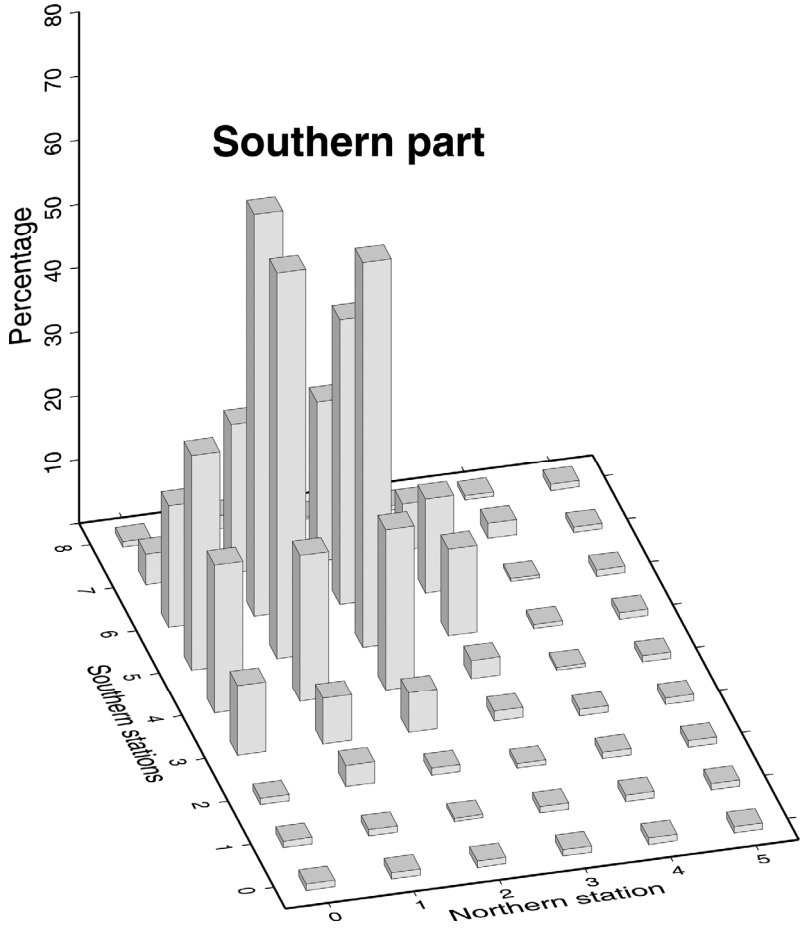

Fig. 5 Relative number of well-located events in the **southern par**t of dataset, shown as a function of the combinations of recording by the southern and northern CRL stations. The values are normalized to 500 events to compensate for different number of epicenters in the individual epicentral areas, while keeping characteristics of the whole data set.

2 stations on the north, together with 2, 3, or 4 stations on the south, etc. The overview of such combinations is given separately for the southern, central and northern part of events in Figures 5, 6 and 7. The higher number of southern stations seems to prevail over the number of northern stations in almost all of combinations, even for the northern part of events. But we have to remark that only *P*-wave onsets are taken in consideration in these Figures and that the weight of individual stations could not be taken into account.

From the Figures we can see, that whereas for the southern group of epicenters we can get a significant number of locations (over 30) using just the combination of southern stations, for the central and northern part we need to use combinations including at least two northern stations (mostly PSA and TRI).

COMPARISON WITH THE NOA LOCATION

It may be interesting to compare the CRL locations with those of the regional Greece agency NOA. For the study region and temporal window, the catalog of NOA (http://www.gein.noa.gr/services/info-en.html) comprises 121 events. Their magnitudes vary from 2.6 to 4.1. From these 121 events only 95 can be associated with the CRL events according their origin times. The mean distance between the CRL and NOA epicenter is 11.7 km, but in one case the distance amounts to as much as 46 km (Figure 8). Moreover, the associated events show a systematic difference in magnitude: 0.5 units larger in NOA catalog, on average, excluding cases of negative CRL magnitudes; see Figure 9. The very low magnitude values (including negative ones), reported for some events by CRL, are missing in the NOA data.

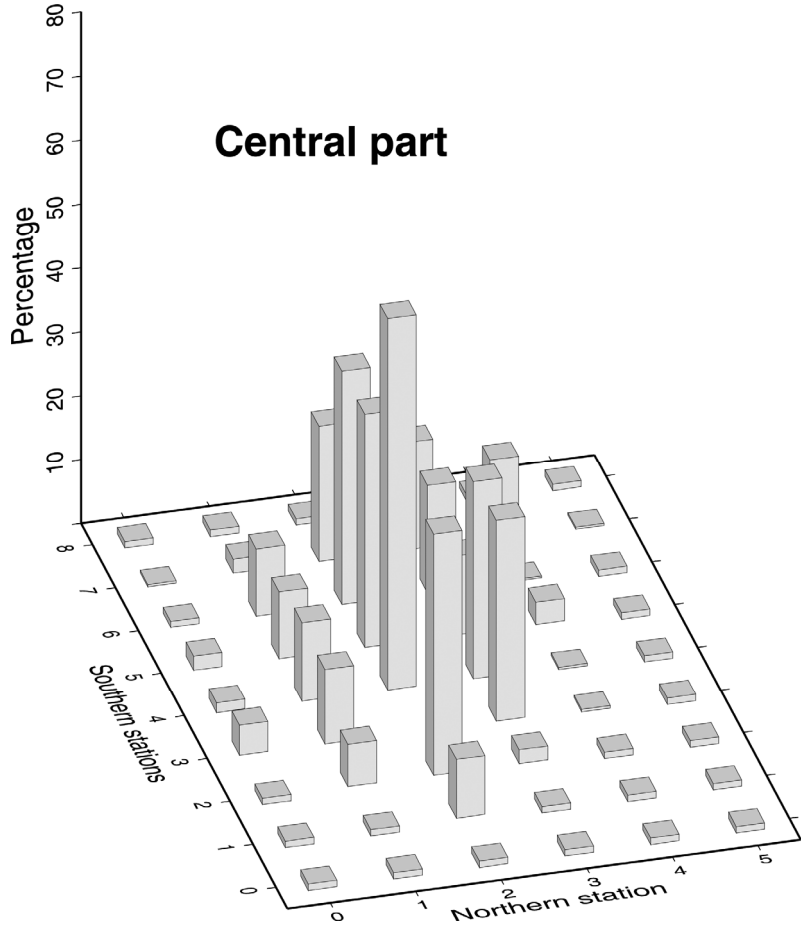

Fig. 6 As in Figure 5, but for the **central part** of dataset.

In summary, NOA proves to be able to monitor activity of the studied region down to relatively small magnitudes. On the other hand, both epicenter positions and magnitude values reflect the fact that CRL is a specifically targeted and relatively dense local network. In spite of the critical evaluation of some CRL stations in the preceding sections, this network as a whole is well suited for the detailed studies.

CONCLUSION

This study revealed an unequivocal heterogeneity in the efficiency of the seismic stations operating within CRL network in the western part of the Corinth Gulf. For a detailed classification, see Figures 2, 3, 4 and Figures 5, 6, 7. For a simple summary, let us consider a threshold, for example the 40% weighted recording percentage. Without considering the epicentral area, i.e. taking the whole set of epicenters and *P*-wave onsets, only four southern stations AGE, AIO, DIM and TEM, and one northern station PSA fulfill this limit. For the central and northern epicentral area this condition is fulfilled as well by southern station ALI and by the northern station TRI. For the southern area, the condition is fulfilled by station LAK and KOU. Under stations with very low efficiency for all the three epicentral areas we identify the northern stations KAL, PAN, PYR, DAO, DAF and SER. For the southern area of epicenters we can further add the stations ALI and ELE, and for the northern part of epicenters the station LAK.

The practical significance of the results is obvious. In future development of the network in the Gulf the most efficient stations should be kept, or further improved as regards the sensors, telemetry, etc. What is behind the low efficiency of some stations is a difficult question, beyond the scope of this study. For some of them the weak performance might be shown to relate with local geology (see, e.g. Armijo et al., 1996), thus impossible to improve. However, some stations might improve their behavior quite considerably. This was the case of SER station, upgraded in 2007 by a 4-m vault with perfect thermal isolation (in co-operation between the Charles University, Prague, and the University of Patras in the framework of the 3HAZ project).

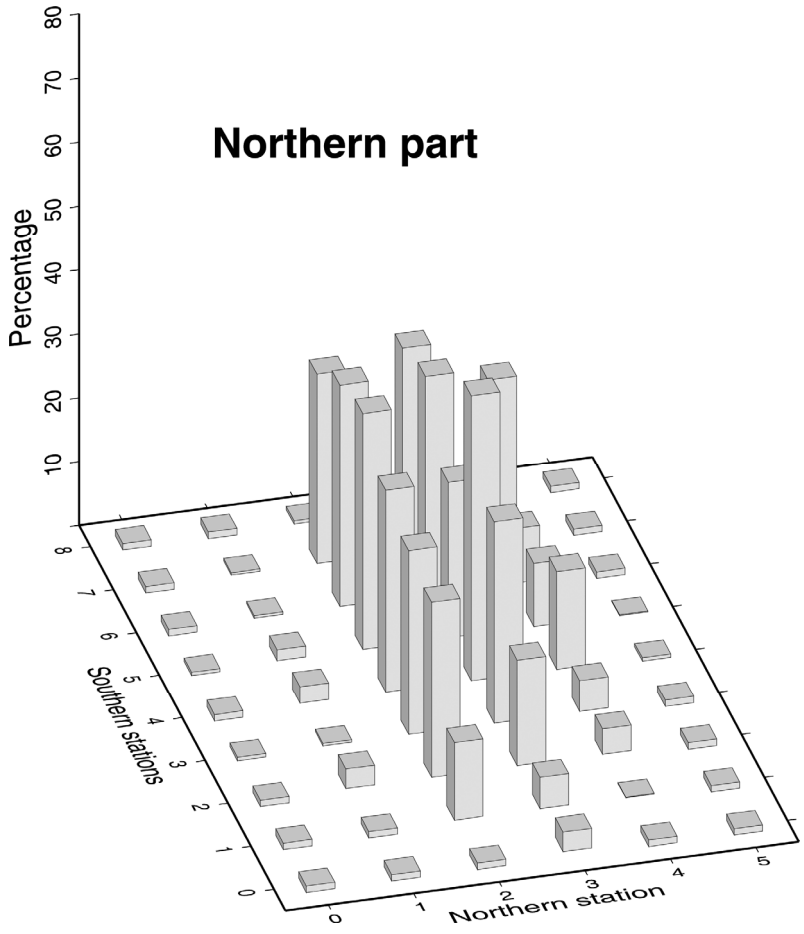

Fig. 7 As in Figure 5, but for the **northern part** of dataset.

ACKNOWLEDGEMENTS

We highly appreciate the set of CRL network station data (*P* and *S* readings) that was provided to us by Helene Lyon-Caen in the frame of studies incorporated into the 3-HAZ-CORINTH EC project (0004043). We are also thankful to F. Cornet and E. Sokos, for their constructive recommendations that improved results of this paper. This study was partially supported by the following grants in the Czech Republic: GACR 205/07/0502, MSM0021620860.

REFERENCES

Armijo, R., Meyer, B., King, G., Rigo, A. and Papanastassiou, D.: 1996, Quarternaly evolution of the Corinth rift and its implications for the late Cenozoic evolution of the Aegean, Geophys. J. Int., 126, 11–53.

Bernard, P., Lyon-Caen, H., Briole, P., Deschamps, A., Boudin, F., Makropoulos, K., Papadimitriou, P., Lemeille, F., Patau, G., Billiris, H., Paradissis, D., Papazissis, K., Castarede, H., Charade, O., Nercessian, A., Avallone, A., Zahradnik, J., Sacks, S. and Linde, A.: 2006, Seismicity, deformation and seismic hazard in the western rift of Corinth: New insight from the Corinth Rift Laboratory (CRL), Tectonophysic*s*, 426, 7–30.

Lee, W.H.K. and Valdés, C.M.: 1989, Hypo71PC. Toolbox for seismic data acquisition, processing, and analysis, IASPEI & SSA.

Lyon-Caen, H., Papadimitriou, P., Deschamps, A., Bernard, P., Makropoulos, K., Pacchiani, F. and Patau., G.: 2004, First results of the CRLN seismic array in the western Corinth rift: evidence for old fault reactivation, C. R. Geoscience, 336, 343–351.

Rigo, A., Lyon-Caen, H., Armijo, R., Deschamps, A., Hatzfeld, D., Makropoulos, K., Papadimitriou, P. and Kassaras, I.: 1996, A microseismic study in the western part of the Gulf of Corinth (Greece): implications for large scale normal faulting mechanisms, Geophys. J. Int. 126**,** 663–688.

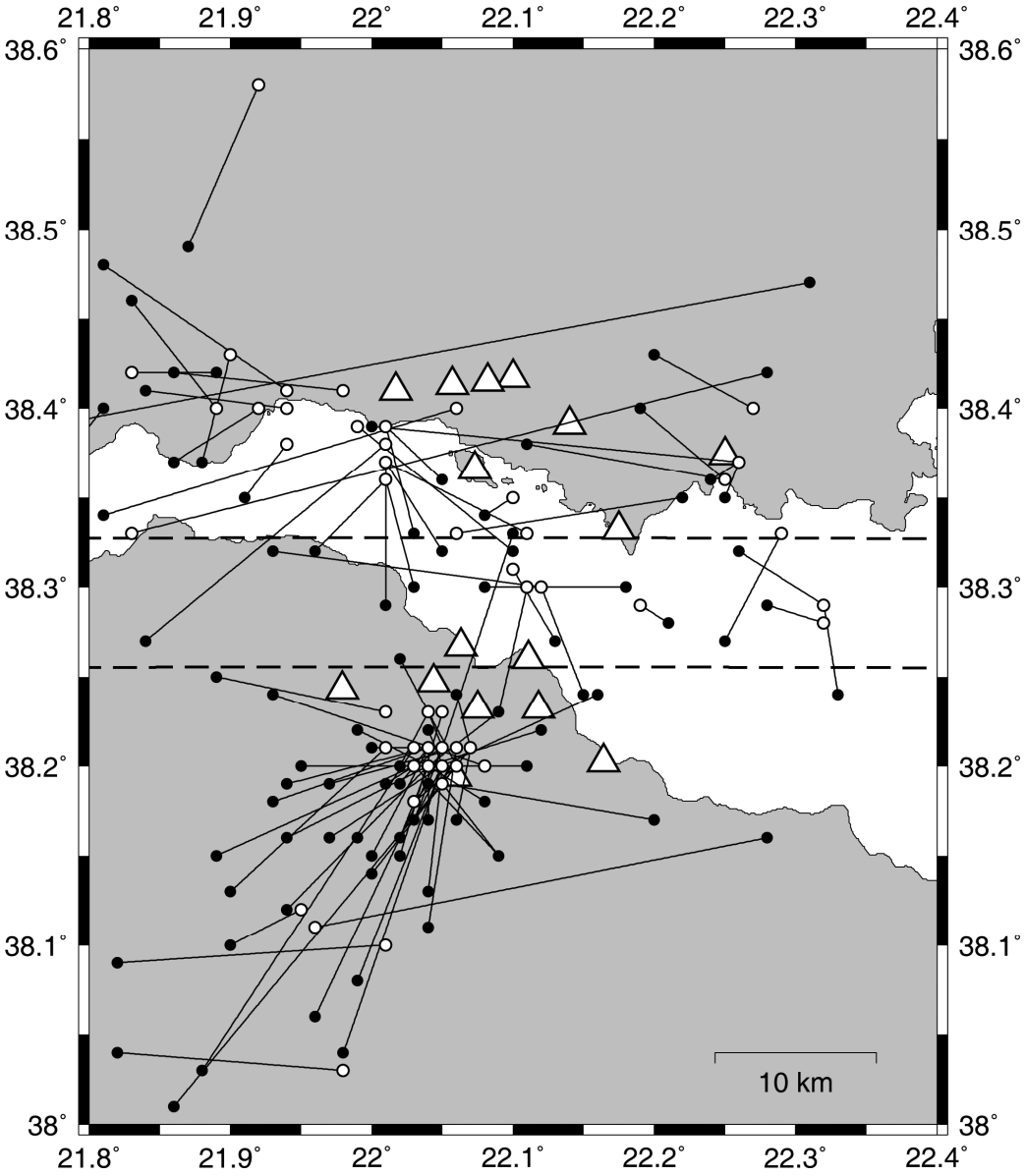

Fig. 8 Corresponding CRL (circles) – NOA (dots) locations pairs of 95 events connected by lines. Triangles show the position of CRL stations. Dashed lines are the same as in Figure 1.

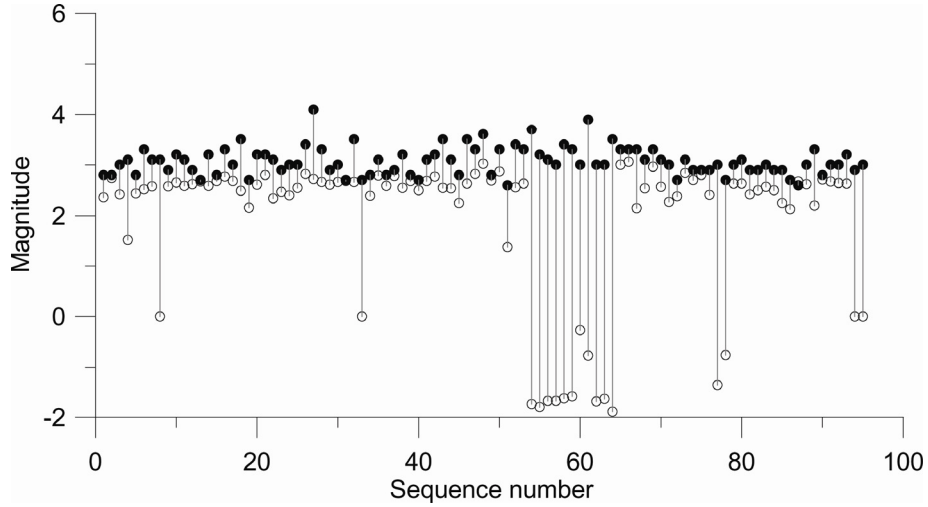

Fig. 9 Comparison of magnitudes for CRL – NOA location pairs of 95 events, Corresponding magnitudes are connected by line. CRL magnitude (duration) – circles, NOA magnitude (mainly Lm) – dots.